Drug loaded bi-layered sponge for wound management in hyperfibrinolytic conditions

Article *in* Journal of Materials Chemistry B · June 2015

DOI: 10.1039/C5TB00568J

CITATIONS
26

READS
279

6 authors, including:

Nimal Raveendran
The University of Queensland
16 PUBLICATIONS **543** CITATIONS
SEE PROFILE

Sahadev Shankarappa
Amrita Institute of Medical Sciences
37 PUBLICATIONS **1,367** CITATIONS
SEE PROFILE

Raja Biswas
Amrita Institute of Medical Sciences
115 PUBLICATIONS **5,483** CITATIONS
SEE PROFILE

Journal of
Materials Chemistry B

PAPER

Cite this: J. Mater. Chem. B, 2015, 3, 5795

Drug loaded bi-layered sponge for wound management in hyperfibrinolytic conditions

Annapoorna Mohandas,† T. R. Nimal,† Vishnu Das,† Sahadev A. Shankarappa, Raja Biswas and R. Jayakumar*

Received 30th March 2015,
Accepted 9th June 2015

DOI: 10.1039/c5tb00568j

www.rsc.org/MaterialsB

Excessive bleeding due to premature clot lysis and secondary bacterial wound infection are two significant problems that contribute to increased morbidity in patients with hyperfibrinolytic conditions. In this study, we have developed a bi-layered sponge that promotes fibrin clot stability and prevents secondary bacterial wound infections. Using the technique of freeze-drying, a bi-layer matrix consisting of hyaluronic acid (HA) containing aminocaproic acid (amicar) and chitosan containing tetracycline loaded *O*-carboxymethyl chitosan nanoparticles (Tet-*O*-CMC NPs) were produced. We hypothesized that the top chitosan layer with Tet-*O*-CMC NPs will prevent wound infection and concomitantly act as a matrix for cellular migration and subsequent wound healing, while the amicar-containing layer would promote clot stability. Tet-*O*-CMC NPs and bi-layer sponges were characterized using Dynamic Light Scattering (DLS), Scanning Electron Microscopy (SEM) and Fourier Transform Infra Red (FT-IR) spectroscopy. Physiochemical characterization such as porosity, swelling and mechanical testing was performed. The drug release study shows that the bi-layered sponge demonstrates a robust burst release of amicar and a sustained release of tetracycline. The *ex vivo* muscle permeation study indicated that Tet-*O*-CMC NPs have enhanced tissue permeation compared to free Tet. *In vitro* antibacterial activity of the bi-layer sponge towards laboratory and clinical strains of *Staphylococcus aureus* and *Escherichia coli* was proved. The *ex vivo* bacterial sensitivity study using porcine muscles confirmed the antibacterial activity, while the cell viability study using human dermal fibroblast (HDF) cells revealed its biocompatible nature. The *in vitro* antifibrinolytic study shows that the bi-layered sponge with amicar showed significant protection against streptokinase induced clot lysis. These studies suggest that the prepared amicar and tetracycline loaded chitosan–HA bi-layered sponge can be used effectively to promote better wound healing by simultaneously preventing bacterial infection, and enhancing clot stability.

Introduction

Hyperfibrinolysis is a devastating clinical condition that is characterized by uncontrolled and catastrophic bleeding.[1] Liver disorders, severe trauma, major surgical procedures, and certain congenital conditions are some of the known causes of hyperfibrinolysis.[2] Inability to sustain a stable clot and enhanced clot lysis leads to profuse bleeding from wounds, making routine wound management difficult. While management of excessive bleeding from wounds is challenging, an overlying secondary bacterial infection further complicates wound care. *Staphylococcus aureus* (*S. aureus*), *Pseudomonas aeruginosa* and *Escherichia coli* (*E. coli*) are some common bacteria responsible for secondary bacterial infection of wounds.[3] Hence, in clinical conditions where hyperfibrinolysis and secondary bacterial infection co-exist, a combinatorial therapeutic strategy would be more effective.

One of the fundamental mechanisms responsible for clot lysis in hyperfibrinolytic conditions is the enhanced conversion of the anti-clotting factor, plasminogen (PA) to plasmin, by the enzyme tissue plasminogen activator (t PA).[4,5] Degradation of fibrin and subsequent dissolution of the clot occurs as a direct activity of plasmin at the site of the wound. Currently, one of the drugs used to manage excessive bleeding due to hyperfibrinolysis is aminocaproic acid (amicar®), a lysine analogue that binds to plasminogen and prevents plasmin induced clot lysis.[6] One possible therapeutic option to control bleeding from wounds in hyperfibrinolytic conditions could be the use of aminocaproic acid incorporated degradable polymeric matrices that could be clinically used as bandages. Additionally, inclusion of an antibiotic within the polymeric matrix would have the added advantage of preventing bacterial complication within the wound site. Among the commonly used antibiotics, tetracycline has a broad range of anti-bacterial activity and it has been previously demonstrated that tetracycline in a nanocarrier like

Amrita Centre for Nanosciences and Molecular Medicine, Amrita Institute of Medical Sciences and Research Centre, Amrita Vishwa Vidyapeetham University, Kochi-682041, India. E-mail: rjayakumar@aims.amrita.edu, jayakumar77@yahoo.com; Fax: +91 484 2802020; Tel: +91 484 2801234
† Authors contributed equally.

O-CMC (*O*-carboxymethyl chitosan) exhibits improved activity, penetration, and has a sustained release profile.[7]

Natural polymers like chitin, chitosan, cellulose, alginate, and hyaluronic acid are some of the more preferable and robust materials for use as drug delivery matrices.[8,9] Chitosan has antibacterial, anti-inflammatory and haemostatic properties, which favor its applications in wound healing.[9–11] Although chitosan is reported to have antibacterial activity, its activity is pH dependent and shows minimal antibacterial activity in neutral pH. It can be enhanced by the incorporation of antibacterial drugs/nanoparticles into chitosan.[12] Chitosan, the de-acetylation product of chitin degrades into its monomer *N*-acetyl-β-D-glucosamine that has several functions in wound healing. Chitosan has the ability to enhance fibroblast proliferation, simulate type IV collagen synthesis, activate polymorphonuclear cells, modulate cytokine production, and stimulate giant cell migration in wounds.[9–11] Additionally chitosan serves as an excellent drug loadable matrix that can be used to produce prolonged drug release.[13]

However, the slow degrading nature of chitosan in comparison to copolymers such as hyaluronic acid (HA) demonstrates a reduced burst release of loaded drugs.[14] HA, a copolymer of *N*-acetyl glucosamine and glucuronic acid is the chief component of the extra cellular matrix (ECM).[15] Due to its non-immunogenic and viscoelastic behavior, HA is a suitable biocompatible material in wound management.[16] Additionally, the by-products of HA degradation has been shown to facilitate fibroblast proliferation and angiogenesis.[16] Furthermore, HA provides a moist environment and prevents dryness of the wounded tissue surface and promotes healing by increasing collagen secretion at the wound site by fibroblast proliferation.[16]

In this study we fabricated a dual functional bi-layered sponge with anti-fibrinolysis and antibacterial properties. The anti-fibrinolytic, aminocaproic acid was loaded onto the fast releasing HA, while the antibacterial Tet-*O*-CMC NPs were loaded onto the sustained releasing chitosan matrix. The goal of the study was to develop a multifunctional sponge that could be used as a therapeutic bandage in the management of wounds in patients with hyperfibrinolytic conditions. Fig. 1 shows the schematic representation of the bi-layered sponge.

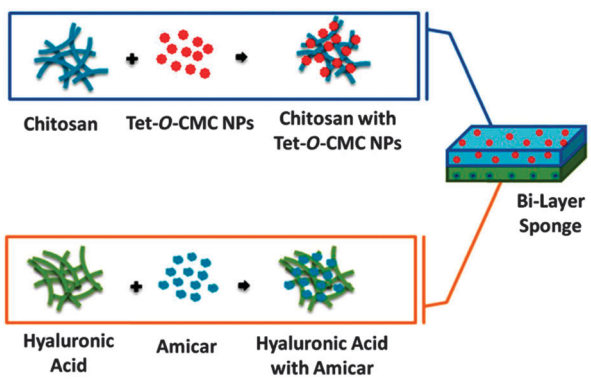

Fig. 1 Schematic representation of layers in bi-layer sponge.

Experimental

(a) Materials

Chitosan (M_W 100–150 kDa), (degree of deacetylation – 85%) and *O*-CMC sodium salt (degree of deacetylation – 61.8% and degree of substitution – 54%) were purchased from Koyo Chemical Ltd (Japan). HA was purchased from Qingdao Haitao Biochemical Co Ltd (China). Tetracycline hydrochloride was purchased from HiMedia. Acetic acid and sodium hydroxide were purchased from Qualigens, India. 6-Amicar was obtained from Sigma-Aldrich. Streptokinase was purchased from Gland Pharma Limited. Luria Bertani broth (LB broth) and Agar-Agar were purchased from Himedia, India. Alamar Blue, Trypsin-EDTA, DAPI, antibiotic antimycotic solution, Minimum Essential Medium (MEM), and Fetal Bovine Serum (FBS) were obtained from Gibco and Himedia, India. All chemicals were used with no further purification.

(b) Bacterial strains and culture conditions

S. aureus strain SA113 (ATCC 35556)[17] and *E. coli* strain (ATCC 25922) were used for this study.[18] In liquid culture, all bacterial strains were cultured aerobically in LB broth at 37 °C with shaking at 160 rpm.

(c) Cell culture

A normal human dermal fibroblast (HDF) cell line was purchased from Promocell. For the cell viability study HDF cells were cultured in MEM and supplemented with 10% FBS and 1% antibiotic antimycotic solution.

(d) Preparation of chitosan hydrogel

Chitosan hydrogel was prepared by neutralizing 2% chitosan solution with 1% NaOH.[19] The obtained hydrogel was washed 3 times with double deionized water before use.

(e) Preparation of amicar–HA hydrogel

2% HA solution was prepared by dissolving HA in distilled water by vigorous stirring under room temperature. 2% amicar was measured and added into the HA solution and stirred for 1 h to dissolve the drug homogenously.

(f) Preparation of Tet-*O*-CMC NPs

Tet-*O*-CMC NPs were synthesized by ionic cross-linking of *O*-CMC using calcium chloride as a cross-linker as previously reported by our group.[7]

(g) Incorporation of Tet-*O*-CMC NPs into chitosan hydrogel

The prepared Tet-*O*-CMC NPs were then re-suspended in double distilled water which was then added drop wise into 2% chitosan hydrogel under constant vigorous stirring. Tet-*O*-CMC NPs were uniformly homogenised with chitosan hydrogel and were used for the preparation of bi-layer sponge after lyophilisation.

(h) Preparation of bi-layer sponge

Initially, a homogenized amicar–HA hydrogel mixture was poured on to a Teflon mould and stored at −20 °C overnight.

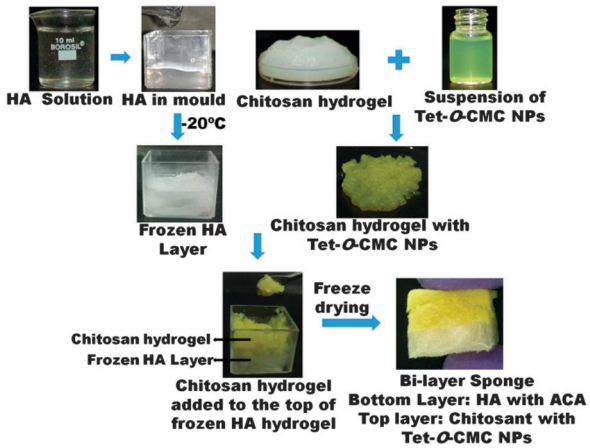

Fig. 2 Schematic representation of preparation of bi-layer sponge.

After freezing, the mould was taken and the top of HA–amicar hydrogel (bottom layer) was obtained. Chitosan hydrogel with Tet-*O*-CMC NPs was spread and kept for 20 min at room temperature. The mould with hydrogels was stored at −20 °C overnight. The frozen samples were lyophilized (Martin Christ, Germany) for 24 h to obtain porous bi-layer sponge with a top layer of Tet-*O*-CMC NPs incorporated into the chitosan sponge layer and the bottom layer of HA sponge containing amicar (Fig. 2).

(i) Nanoparticle size analysis and characterization

Particle size, particle size distribution and zeta potential were analyzed by DLS (Malvern Zeta Sizer, Nano series). The surface charge and stability of the same were also analyzed using the same system. The average size and surface morphology were studied using SEM (JEOL JSM-6490LA Analytical SEM). The Tet-*O*-CMC NP suspension was diluted 5 fold with double distilled water and dropped on an aluminium stub and sputter coated with gold using an automatic fine gold coater (JEOL JFC-1600) at 10 mA for 120 s and then scanned for SEM images. FT-IR analyzed potential chemical interactions between the constituents within the nanoparticle system. FT-IR spectra of *O*-CMC NPs were compared to Tet-*O*-CMC NPs.

(j) Encapsulation efficiency (EE)

The supernatant obtained after particle separation from the reaction mixture was collected and quantified using a UV spectrophotometer (UV-1700 Pharma Spec, Shimadzu) at 275 nm. The encapsulation efficiency of the Tet-*O*-CMC NPs was calculated using the formula:

$$\mathrm{EE}\% = \frac{(\text{Total amount of Tet added} - \text{Free Tet})}{(\text{Total amount of Tet added})} \times 100$$

(k) Characterisation of bi-layer sponge

Lyophilized samples were cut into thin layers and placed on an aluminium stub using carbon tape and sputter coated with gold for SEM imaging. SEM (JEOL, JSM-6490LA, and Japan) was employed to observe the morphology of prepared sponges. The characteristic peaks of chitosan, HA, amicar, tetracycline, *O*-CMC, and Tet-*O*-CMC NPs were obtained by Fourier transform infrared spectroscopy (FT-IR) (Perkin-Elmer Co. Model SPECTRUM RXI, FT-IR).

(l) Porosity evaluation

The porosity of the sponges (average void volume) was studied using the alcohol displacement method.[20] Chitosan bandage was taken as control and all the samples were in triplicate. Sponges of uniform size and shape were made using a scaffold punch. Dimensions of the sponges were measured using a vernier calliper and the volume was calculated. The displacing liquid was ethanol. The initial weight of sponges (dry weight) was measured and immersed in a known volume of absolute ethanol and allowed to penetrate into the porous sponge for 24 h. Final weights (wet weight) of the sponges were noted down and porosity was calculated using the equation below.

$$\%\ \text{Porosity} = \left[\frac{(W_\mathrm{f} - W_\mathrm{i})}{\rho V}\right] \times 100$$

where, W_i = initial weight of the sponge (dry weight), W_f = final weight of the sponge (wet weight), ρ = density of absolute ethanol (constant), V = volume of sample before immersion in alcohol.

(m) Swelling and water uptake studies

The swelling study was carried out in PBS. Double distilled water was used for the water uptake studies. Water uptake ability of the sponges was also studied. Lyophilized samples were cut into uniform size and shape using a scaffold puncher and triplicates were used for the study. The initial weight of the samples was noted and immersed in PBS buffer/water and samples were placed at 37 °C for incubation. At different time points samples were taken out and the wet weight was measured after removing the excess PBS/water content by using a filter paper. The buffer/water uptake was analysed by the formula.

$$\text{Swelling ratio} = \left[\frac{(W_\mathrm{w} - W_\mathrm{i})}{W_\mathrm{i}}\right] \times 100$$

where, W_i = initial weight of the sponge (dry weight) and W_w = final weight of the sponge (wet weight).

(n) Tensile strength and % elongation evaluation

Mechanical properties of the sponges were evaluated by measuring tensile strength and % elongation. The specimens were prepared by cutting it into a rectangular block of dimensions 50 mm × 10 mm × 2 mm. The specimens were clipped with a special pneumatic gripper on both ends. Samples were triplicated for the study. The tensile strength and percentage of elongation at break were measured using a universal testing machine (Tinius Olsen) with a load cell of 250 N, a crosshead speed of 25 mm h^{-1} and a gauge length of 5 cm at room temperature. The values of both tensile and % elongation at break were noted. Bare chitosan sponge was taken as the control sample and the mechanical properties were compared with bi-layer sponge.

(o) Cell viability

Cell viability of the prepared Bi-layer sponges on HDF cells was studied using Alamar Blue Assay.[21] Sponges were cut into uniform

size and shape using a scaffold puncher and sterilized by ethylene oxide gas. 10 000 HDF cells were seeded per well of a 96 well plate on sterile sponges and were incubated for up to 48 h. After 24 h and 48 h the culture medium was replaced with 10% alamar blue in MEM and incubated for 4 h. After the incubation period the optical density (O.D) was measured using a micro plate spectrophotometer reader (BiotekPowerWave XS, USA) at 570 nm, with 620 nm set as the reference wavelength. HDF alone was used as positive control and Triton X100 treated cells were used as negative control. The percentage of cell viability is calculated by using the formula:

$$\text{Cell viability (\%)} = \frac{\text{O.D of test sample at 570 nm} - \text{O.D of test sample at 600 nm}}{\text{O.D of positive control at 570 nm} - \text{O.D of positive control at 600 nm}} \times 100$$

(p) *In vitro* drug release study and its kinetic modelling

The *In vitro* drug release study was carried out at pH 7.4. Chitosan sponge with Tet-*O*-CMC NPs and HA with amicar was used for the drug release study. Samples were cut into a uniform size and shape using a scaffold puncher in triplicates. Samples were soaked in 5 ml PBS and incubated at 37 °C under gentle shaking. At different time intervals a known volume of buffer was withdrawn and the drug release was quantified spectrophotometrically. Drug release % was quantified using the formula:

$$\%\ \text{Drug release} = \left[\frac{(\text{drug released at definite time})}{\text{total amount of drug in the sponge}}\right] \times 100$$

To interpret the release mechanism of the drugs, kinetic modeling was done.

(q) Antifibrinolytic activity study

Citrated blood was collected from blood bank of Amrita Institute of Medical sciences and Research, Kochi, India. The blood was transferred to a micro centrifuge tube containing different units of streptokinase (0, 10, 100 and 1000 IU) and bi-layer sponge with/without amicar. Streptokinase is a plasminogen activator, that mimic hyperfibrinolytic condition *in vitro*. The unit of streptokinase which caused complete lysis was optimised for further studies. The coagulation pathway was initiated with the addition of 50 μl of 5% calcium chloride solution into 500 μl of citrated blood, followed by incubation at 37 °C water bath for 15 min. After the incubation the serum is removed to measure the clot weight and was compared with controls. PBS and different units of streptokinase were used as negative control and tubes without streptokinase and amicar serves as positive control.

(r) *In vitro* antibacterial activity assessment

McFarland standard 0.5 ($\sim 10^8$ CFU ml^{-1}) was set and an aliquot of the *S. aureus* and *E. coli* suspension was added to the test tubes that contains 8 ml of LB broth containing pre-sterilized samples (10×5 mm^2) to get a dilution of $\sim 10^6$ CFU ml^{-1}. Test tubes were incubated at 37 °C in a shaking incubator. After incubation, LB broth containing bacteria were serially diluted in sterile saline and plated onto LB agar plates. The number of bacterial colonies was counted and plotted for quantification.

(s) Validation of antibacterial activity against clinical isolates

As described above antibacterial activity assessment against clinical isolates of *S. aureus* and *E. coli* was performed. The turbidity formed after incubation period of 12 h was measured by taking absorbance at 580 nm.

(t) *Ex vivo* antibacterial activity study

The antibacterial activity of bi-layer sponge was analyzed using porcine muscles. The overnight cultures of *S. aureus* and *E. coli* were centrifuged at 5000 rpm for 10 min and washed two times with sterile PBS. The bacterial cells were finally re-suspended in 1 ml sterile PBS for the study.

Fresh hind limb muscles were cut into 1 cm^3 blocks and placed in 12 well plates. The muscles were infected by injecting 50 μl of the inoculums at the center of blocks by using a 1 ml syringe. 1 cm^2 chitosan-HA bi-layer sponge with and without Tet-*O*-CMC NPs was used for the study. The hydrated samples were placed on the infected muscle. 1 ml of Sterile PBS was added to each well to avoid dehydration during the experiment. The entire system was incubated at 37 °C for 7 h. Post incubation, the muscle tissue was isolated and minced into small pieces using a sterile surgical blade. The minced homogenate was transferred into a conical tube containing 10 ml sterile PBS, vortexed vigorously and plated on LB agar plates in serial dilutions. The reduction in bacterial colonies was quantified.[22]

(u) *Ex vivo* muscle permeation studies

Nanoparticles released from the dressing material need to be penetrated through the muscles to avoid the deep tissue infections in open wounds. The Franz diffusion cell apparatus was used to study the penetration of nanoparticles across tissue samples.[23] Human muscles and porcine hind limb muscles share physiological similarities. Porcine muscles were collected from local slaughterhouse immediately after butchering. The white fat layers was removed from the collected sample, washed thoroughly with double distilled water and was kept in normal saline to maintain the osmotic balance of the tissues.

The Franz diffusion cell apparatus has two compartments – donor and receptor. The receptor chamber volume varied from 7.0 to 7.4 ml and the area for diffusion was 2.54 cm^2. The compartment was filled with PBS (pH 7.4) and maintained at 37 °C using a circulating water jacket. The receptor media was kept under gentle stirring to maintain mass and heat transfer. Porcine muscles were cut into appropriate size and thickness and kept on the top of the receptor compartment. Chitosan sponges containing Tet-*O*-CMC NPs were used for the study and compared with chitosan sponge containing same amount of tetracycline without any carriers. The dressing materials were clamped tightly to avoid any leakage. 2 ml of PBS was added to the donor compartment to hydrate the dressing material and tissue.

0.5 ml of the acceptor fluid was withdrawn at different time points (1, 2, 3, 6 and 24 h) and replaced with equal volume of PBS. The amount of drug in the withdrawn samples was quantified by taking the UV absorbance at 275 nm using a double beam spectrophotometer. The penetration was analyzed by plotting the cumulative percent of drug permeated per cm^2 *vs.* time.

The muscles after the penetration study were fixed in buffered formalin and 5 μm thick sections were taken using a cryotome (Leica CM 1510 S). The tetracycline fluorescence in the tissue sections was observed under a fluorescent microscope. The auto-fluorescence of the tissue sample has been corrected.

(v) Statistical analysis

The data are expressed as mean ± standard deviation (SD). The Student's *t*-test was conducted to analyze the results statistically. The probability level of $p < 0.05$ was considered to be statistically significant ($^{*}p < 0.05$, $^{**}p < 0.01$ and $^{***}p < 0.001$).

Results

The particle size distribution of Tet-*O*-CMC NPs in aqueous medium was determined using the DLS technique, and was found to be in the size range of 200 ± 63 nm with mono-dispersion. The zeta potential of Tet-*O*-CMC NPs was −30 ± 5 mV which confirms the stability in aqueous media. The particle size and morphology as analysed from the SEM image ensured the average particles to be in the range of 200 nm with a spherical shape (Fig. 3A). The entrapment efficiency of the prepared Tet-*O*-CMC NPs was calculated using the formula, and was found to be about 64 ± 8%.

Bi-layer sponge characterized using SEM showed well adhered layers of chitosan and HA with interconnected pores (Fig. 3D). HA and chitosan concentration was fixed at 2% w/v. Both the sponges showed a pore size of 200–300 μm. Surface roughness is more in chitosan sponge when compared to the HA sponge. The SEM image of chitosan also shows the highly interconnected pores which favor the wound exudate absorption and moisture vapor transmission (Fig. 3B).

Fig. 4A and B shows the FT-IR peaks of chitosan sponge with a Tet-*O*-CMC NP layer and HA layer with amicar respectively. The FT-IR spectra of *O*-CMC showed a broad peak between 3500 and 3000 cm^{-1}, which corresponds to the stretching vibrations of amine and hydroxyl group.[24] The stretching vibrations of protonated amino groups showed a peak of 1629 cm^{-1}.[25] *O*-CMC sodium salt did not show C–O stretching vibration peak at 1740 cm^{-1}.[25]

The peak at 3365 cm^{-1} is equivalent to the hydroxyl group of tetracycline.[26] The stretching of N–H bonds and vibrations of C–N bonds of tetracycline were observed at 1240–1200 cm^{-1}.[26] In the FT-IR of Tet-*O*-CMC NPs the slight broadening in intensity of the peak at 1639 cm^{-1} compared to control *O*-CMC is due to the interaction between *O*-CMC and tetracycline. Chitosan shows its characteristic peak for NH_2 stretching at 3400 cm^{-1}.[27]

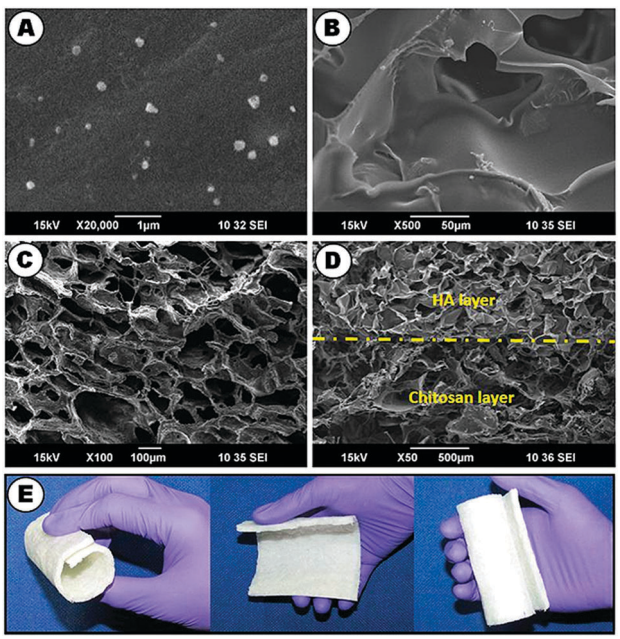

Fig. 3 (A) SEM images of Tet-*O*-CMC NPs, (B) chitosan sponge, (C) HA sponge with amicar, (D) HA and chitosan layers in bi-layer sponge and (E) flexibility and foldability of prepared bi-layer sponge.

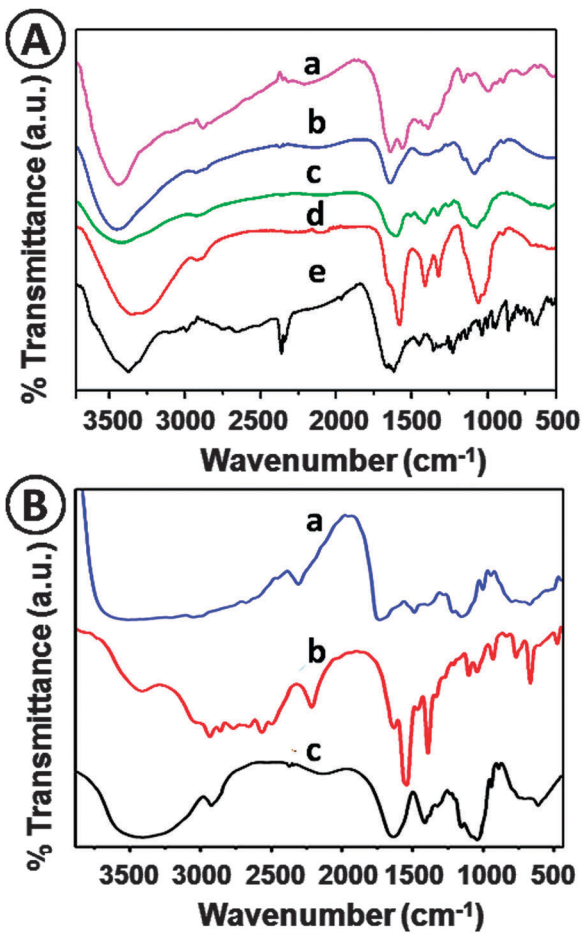

Fig. 4 (A) FT-IR spectra of the chitosan layer in bi-layer sponge- (a) chitosan + Tet-*O*-CMC NPs, (b) bare chitosan, (c) Tet-*O*-CMC NPs, (d) *O*-CMC, (e) tetracycline, (B) the FT-IR spectra of HA layer in bi-layer sponge – (a) amicar in HA, (b) amicar, (c) hyaluronic acid.

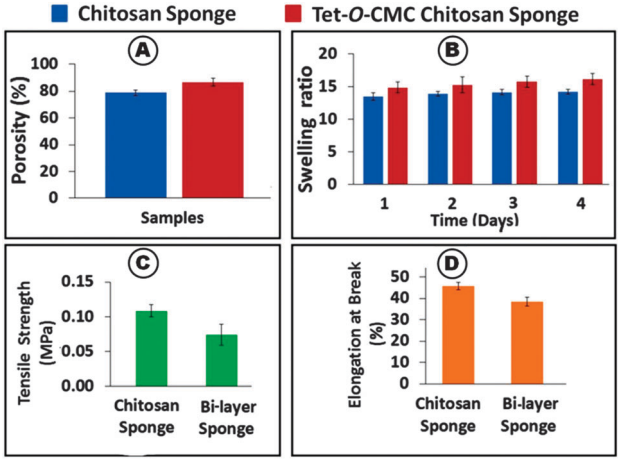

Fig. 5 (A) Porosity studies, (B) swelling studies, (C) tensile strength evaluation and (D) % elongation at break of bi-layer sponge.

The peaks at 1640–1690 and 1035 cm^{-1} correspond to amide I band of chitosan and C–O–C stretching of HA, respectively.[28] Bands at 2850 and 2950 cm^{-1} are due to C–H stretching vibrations of methylene groups of the amicar carbon chain.[29] Two bands at 1530 and 1545 cm^{-1} are attributed to the symmetric and asymmetric stretching vibrations of uncoordinated –COO terminal groups of amicar.[29]

The porosity of the prepared sponges was analysed by a previously reported method.[19] Sponges were taken from the wells containing alcohol and the wet weight was taken, after removing the last drop of alcohol from the sponge. Porosity was found to be 75 to 85% which will help to improve wound exudate absorption capacity (Fig. 5A).[19] Tet-*O*-CMC NPs incorporated chitosan sponge was found to be slightly more porous than the bare chitosan sponge which was not statistically significant.

Fig. 5B shows the swelling studies of the prepared sponges. The study was done by immersing sponges in distilled water and PBS respectively. When compared to the control samples the Tet-*O*-CMC chitosan sponge does not show any significant changes in swelling ability. There was a slight change in the swelling ability of Tet-*O*-CMC chitosan sponge, which may be due to the swelling of *O*-CMC NPs. The remarkable point is that the sponges were saturated with liquid in the first day itself. There was not much significant difference in swelling of sponges after day 1 up to day 4.

Tensile and elongation properties of sponges were analyzed using a universal testing machine. Chitosan sponge used as control sample was compared to bi-layer sponge. Samples were cut into rectangular shape and were hydrated to mimic wound conditions. Fig. 5C shows the tensile strength evaluation data. Chitosan sponge showed a tensile strength of 0.1 MPa whereas the tensile strength of bi-layer sponge was 0.08 MPa, which was adequate for wound dressing material.[13,19]

The percentage of elongation of samples was analyzed in order to evaluate the flexibility and softness of the sponges. Fig. 5D shows the % elongation data of chitosan and bi-layer sponge. Samples were triplicated and hydrated to mimic the wound conditions. Bi-layer sponge and chitosan sponge showed better elongation properties. Both sponges were elongated about 40 ± 5%.

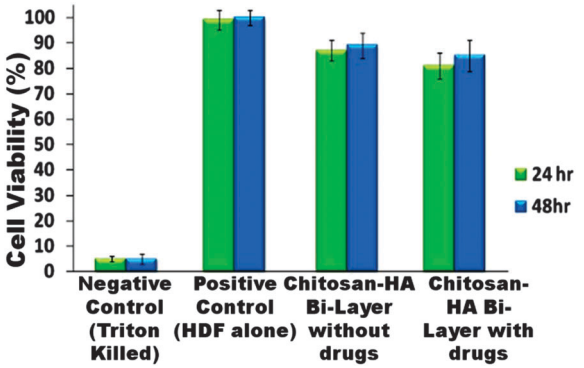

Fig. 6 Cell viability studies using an HDF cell line at 24 and 48 h.

Cell viability studies of bi-layer sponges and control samples were done using alamar blue Assay (Fig. 6). Bi-layer control showed 85–90% viability at 24 h which increased slightly after 48 h. Bi-layer sponge with drugs showed about 81% of cell viability at 24 h and increased to 85% at 48 h. This proved that the bi-layer sponges are non-toxic to the HDF cells.

Fig. 7A and B shows the drug release data of amicar and tetracycline from bi-layered sponge. From the drug release pattern, it was found that 48 ± 5% of the drug was released by 24 h. After that the release pattern is almost slow in a sustained pattern. The sustained dosage of drugs will be helpful in preventing the bacterial infection. Various kinetic models were plotted (Fig. 7C) and from the analysis it was found that the higuchi model shows the closest value to the regression

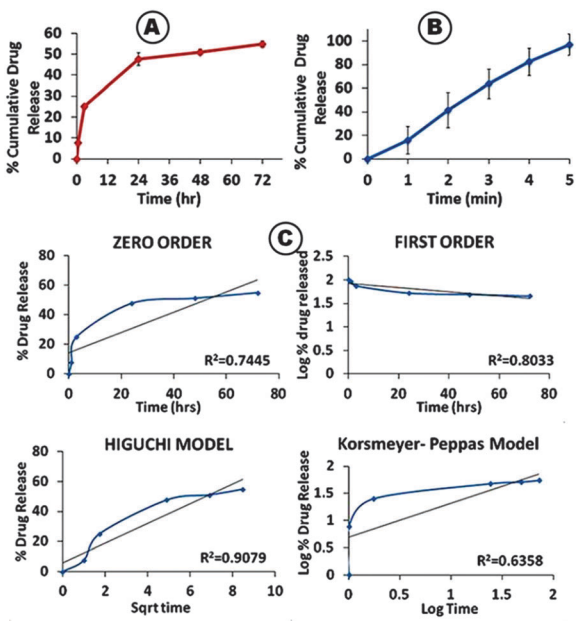

Fig. 7 (A) Drug release study of Tet-*O*-CMC NPs, (B) drug release study of amicar from bi-layer sponge and (C) *in vitro* Tet release data fitted using various kinetic models.

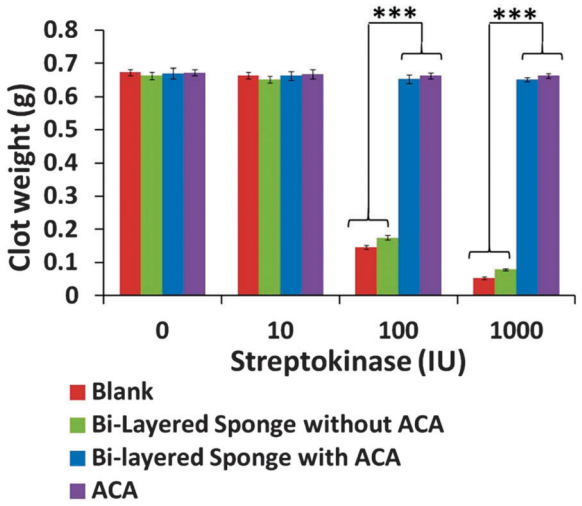

Fig. 8 *In vitro* antifibrinolytic activity of amicar and bi-layered sponge with/without amicar.

coefficient to unity (R^2 = 0.9079). Therefore, the best fit model that fits the drug release of tetracycline is the higuchi model.

The release study of amicar was done in PBS buffer. Fig. 7B shows the percentage cumulative release data of amicar. 96% of amicar from the HA layer got burst released within 5 min.

The antifibrinolytic activity study shows that the developed amicar containing bi-layer sponge showed a significant activity against streptokinase induced hyperfibrinolysis (Fig. 8). 100 IU and 1000 IU of streptokinase treated blood showed a decrease in clot weight but lower concentration *i.e.* 10 IU of streptokinase did not. Bi-layer sponge without any amicar did not stabilize the clot. Whereas, the bi-layer sponge with amicar drug showed excellent clot stability even at higher units of streptokinase treatment. We compared the activity of developed sponge with the same amount of amicar incorporated into the sponge and found that the sponge stabilized the clot similar to that of amicar control. This could be facilitated with the enhanced burst release of amicar from the HA layer that would disintegrate within minutes.

Antibacterial activity of bi-layer sponge having Tet-*O*-CMC NPs was tested against typical Gram positive bacteria *S. aureus* and a gram negative bacteria *E. coli*; which are the major infection causing bacteria. Fig. 9A shows the antibacterial activity evaluation by a serial dilution method. In the figure, samples were indicated from 1 to 10 and top to bottom indicates the colonies of bacteria after serial dilution. The results are represented graphically in Fig. 9B. Bacteria alone were taken as negative control. Chitosan sponge, a bi-layer sponge with amicar did not show any significant activity against both *S. aureus* and *E. coli*. The absence of bacterial colonies illustrates the effective activity of Tet-*O*-CMC NPs released from the chitosan sponge. From the chitosan sponge with Tet-*O*-CMC NPs, tetracycline will be slowly released in a sustained manner which will inhibit the bacterial growth. The O.D values of samples were plotted to note the activity of bi-layer sponge. Fig. 10B shows the antibacterial activity of bi-layer sponge and control samples. The O.D values of nutrient medium containing control samples and bi-layer sponge having Tet-*O*-CMC NPs were

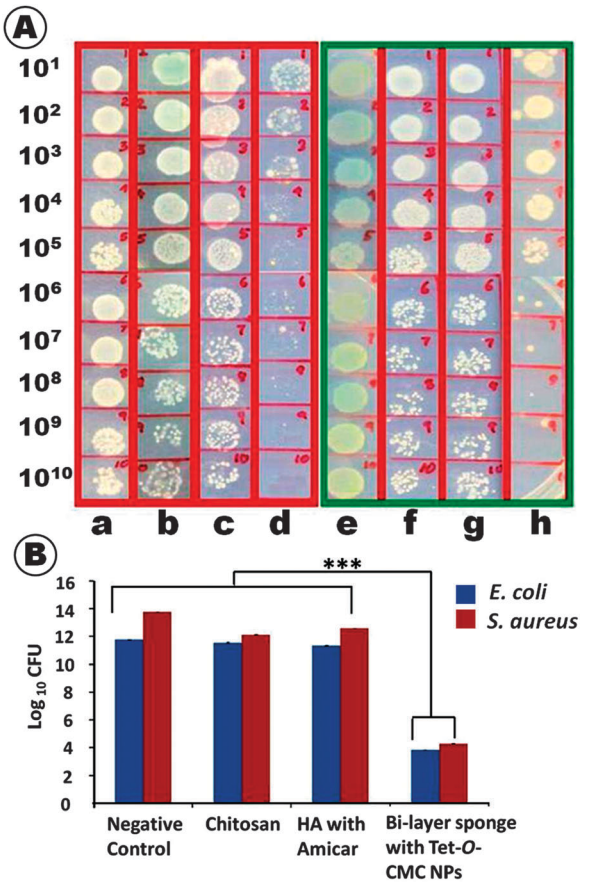

Fig. 9 (A) Antibacterial activity of bi layer sponge against *S. aureus* and *E. coli* by serial dilution method. (a) *E. coli* negative control, (b) chitosan, (c) HA with amicar, (d) bi-layer sponge with Tet-*O*-CMC NPs. (e) *S. aureus* negative control, (f) chitosan, (g) HA with amicar, (h) bi-layer sponge with Tet-*O*-CMC NPs. (B) graphical representation of results obtained after the serial dilution method.

observed. Difference in turbidity was also analyzed visually. Fig. 10A shows the photographs of the test tubes showing difference in turbidity which was clearly visible. More turbidity is due to the higher bacterial growth whereas the clear solution shows lower bacterial growth due to the activity of tetracycline released from the sponges. It was found that the bi-layer sponge with nano tetracycline showed significant reduction in bacterial growth against both *S. aureus* and *E. coli.*

Optical density was measured by the same procedures used for clinical strains. The antibacterial activity of bi-layer sponge against clinical strains (Fig. 11A and B) was studied by measuring the reduction in absorbance at 580 nm. The bi-layer sponge significantly reduced the bacterial growth. Visual analysis also confirmed that the test tubes having bi-layer sponge with Tet-*O*-CMC NPs have lesser turbidity which implies its greater antibacterial activity.

After the *ex vivo* antibacterial study bacterial CFU in muscles were analysed after incubation by plating on LB agar plates (Fig. 12A and B). The results shows that the Tet-*O*-CMC NP encapsulated scaffolds had shown significant reduction in colony forming units in both *E. coli* and *S. aureus* infected muscles.

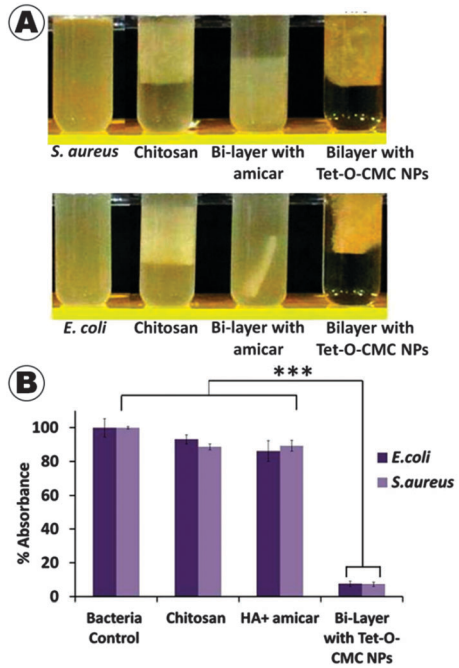

Fig. 10 Antibacterial activity of samples: photograph of tubes after incubation (A) and the percentage of absorbance of the LB broth from the tubes (B).

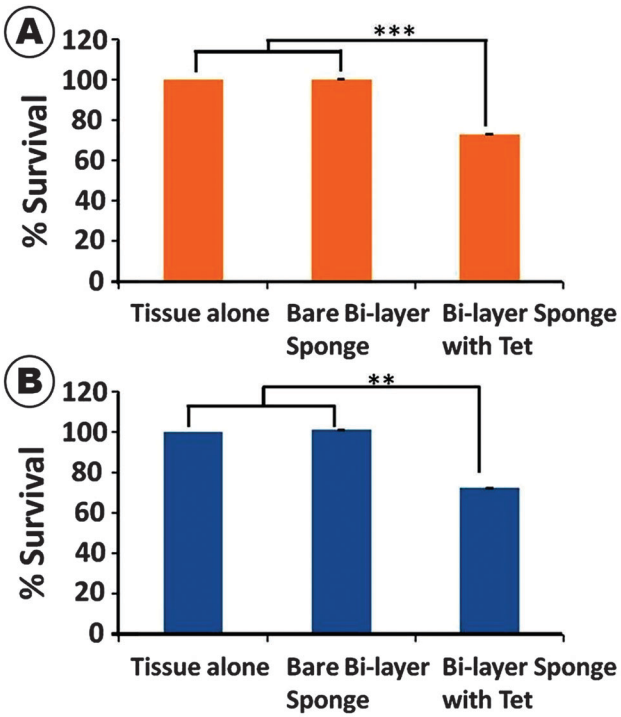

Fig. 12 *Ex vivo* antibacterial study of optimised bandages on porcine muscle infected with (A) *E. coli* and (B) *S. aureus*.

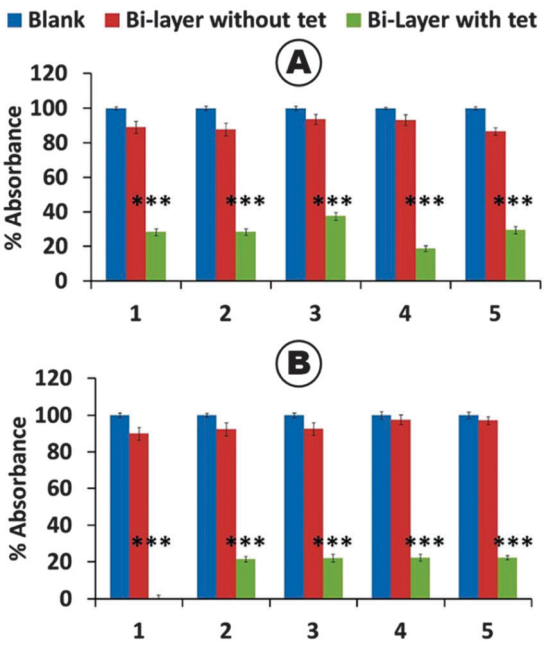

Fig. 11 Antibacterial activity of samples (A and B) against different clinical strains of *E. coli* and *S. aureus* respectively.

The infected muscle treated with bi-layer control had shown a similar concentration as that of the muscle without any treatment.

The cumulative percent of drug permeated per cm^2 was analyzed for both the systems. The kinetics shows that the nanoparticles improved the penetration of tetracycline across the porcine muscle. The penetrated drug reached the receptor compartment within the second hour. Within the first hour, the nanoparticles showed significant penetration. The cumulative percentage of the drug permeated after 24 h was significantly higher in nanoparticle assisted penetration (Fig. 13).

The fluorescent microscopic analysis of the muscle sections after penetration was analysed. The auto fluorescence of muscle was nullified by adjusting the intensity of light exposure and

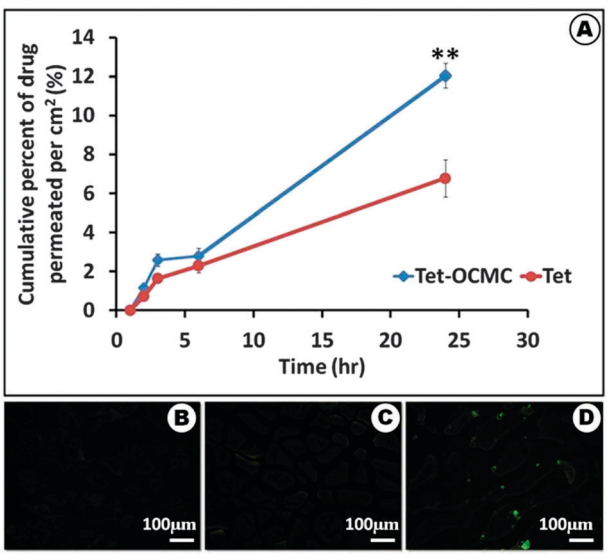

Fig. 13 (A) Drug penetrated across porcine muscle at different time points, *ex vivo* muscle penetration studies of (B) bare porcine muscle section, (C) porcine muscle with bare tetracycline, and (D) porcine muscle section with Tet-*O*-CMC NPs.

all the images were analysed in the same intensity. The image (Fig. 13B–D) shows that the chitosan sponge with bare Tet showed more fluorescence and the boundaries of muscle fascicles were visible. But the nano Tet-*O*-CMC NPs penetrated more as evident in the fluorescent images. The nanoparticles accumulated in the fascicles, showed more fluorescence and can be easily identified.

Discussion

Tet-*O*-CMC NPs were prepared using an ionic gelation method. Concentrations of tetracycline, *O*-CMC, $CaCl_2$ *etc.* were optimized by repeated experimental preparation methods. $CaCl_2$ was used as a cross-linker. From the study it was found that the particle size can be tuned by changing the stirring time, the concentration of cross linker, rpm and temperature. Particle size, stability and drug entrapment also varies with the above mentioned parameters. The size of the Tet-*O*-CMC NPs changes with concentration of the cross-linker added to Tet-*O*-CMC solution. $CaCl_2$ concentration was fixed to 0.1% and was added using a syringe drop wise into the Tet-*O*-CMC solution and was stopped till an opalescent turbid solution is obtained. With increase in the polymer concentration, particle size increases. Particles of smaller sizes were obtained when the polymer concentration was low. Tetracycline which was incorporated into the nano-matrix of *O*-CMC will release the drug in a sustained manner by the degradation of *O*-CMC which further improves the bioavailability of the drug.

From the SEM analysis, the porous nature of sponges was well established. The highly porous nature of the sponge will be beneficial in faster healing of wounds by providing controlled evaporation of wound exudates and their drainage. The porous nature of the bi-layer sponge showed that they can allow better gaseous and nutrient exchange. The chitosan and HA layers in sponges are well adhered. The chitosan layer will remain intact on the top of the wound site after the disintegration of the HA layer. The cytocompatibility assessment of the control and bi-layer sponges using alamar blue assay confirmed the non-toxic nature.

The porosity, swelling and water uptake ability of the bi-layer sponges did not change significantly when compared to the control. The porosity of the sponges has a major role in the swelling and water uptake ability. The data show that the sponges have adequate swelling ability, which will help in absorbing wound exudates and maintaining a moist wound atmosphere at the wound site.[19]

Compared to the bare chitosan sponge, the tensile strength of bi-layer sponge was slightly reduced insignificantly. The reduced tensile value may be due to the soft HA layer, which is highly hygroscopic in nature. Samples were hydrated in order to mimic the wound condition. The disintegration of the HA layer might have slightly reduced the tensile strength. When applying the sponges or bandages in the wounded area, such as in joints flexibility is more important. So from the % elongation data it is clear that the bi-layer sponge is suitable for the wound dressing application in any type of wound surfaces. This more flexible nature will also help to conform on any irregular wound surfaces.

One of the main characteristic of HA is its highly hygroscopic nature, which will easily absorb water and disintegrates quickly.[14] In the bi-layer sponge, the base layer having HA with amicar is designed in such a way that when the sponge is in contact with blood or wound exudate, it will easily disintegrate and provide amicar to the wound site. The release pattern of amicar was found to be an immediate burst release which will be beneficial in a bleeding wound condition. This will help in controlling bleeding and thus minimizing the blood loss through the traumatic wound.

The tetracycline release study shows a sustained slow drug release. The surface bound drug got released at a faster rate which is attributed to initial burst release. The slower drug release of the antibacterial drug at the wound site will help in the prevention of bacterial growth. Reports suggested that Tet-*O*-CMC NPs are endocytosed by phagocytic cells and the colloidal carriers are degraded in endosomes by lysosomal esterases.[7] The problems associated with over dosage can also be minimized by the slow release of tetracycline. Drug release kinetics of Tet-*O*-CMC NPs were also studied by plotting various kinetic models and checked for the best fit model by closeness of the coefficient regression value to unity. From the analysis it was found that Tet-*O*-CMC NPs follow the higuchi model. Here drug release is directly proportional to the square root of time and the release happens at a slower rate. This model is based on Fick's laws of diffusion, where the drug which is incorporated into the porous matrix is dissolved and diffused by solvent. In an ideal case, controlled drug delivery systems are designed in such a way that, the drug delivery can be achieved in a controlled rate in a preferred duration. This will help in improving the efficacy of the drug and ensures safety. The highly porous nature and enhanced swelling ability of the bi-layer sponges results in a better drug release of Tet-*O*-CMC NPs as described in the higuchi model.

The *in vitro* fibrinolytic study showed that, 100 and 1000 IU of streptokinase induced lysis of blood clot *in vitro*. The streptokinase enhances the conversion of plasminogen to plasmin which cleaves the fibrin networks. Sponge without amicar did not show any antifibrinolytic activity. But the amicar loaded sponges showed a significant increase in blood clotting similar to bare amicar. The peculiarity of the prepared bi-layer sponge lies in the immediate release of amicar from the HA layer that would favour the inhibition of plasmin formation similar to amicar control. Amicar released from sponges binds reversibly to the kringle domain of plasminogen and blocks the binding of plasminogen to fibrin and its activation to plasmin.[5]

It was reported that tetracycline has greater activity against both gram positive and gram negative bacteria such as *S. aureus* and *E. coli*.[30] The serial dilution and turbidity assessment showed that bi-layer sponge with nano tetracycline effectively reduced the bacterial colony formation of ATCC and clinical strains of *S. aureus* and *E. coli*. Bacterial turbidity can be seen from the test tubes, but the tubes that contain bi-layer sponge with Tet-*O*-CMC NPs showed clear medium, which proves that they have very good activity against bacterial growth. Nano tetracycline from the bi-layer sponge would interact with the

surface of the bacteria, and the encapsulated tetracycline will be released. Tetracycline is known to inhibit the protein synthesis in bacteria, and thus prevents the bacterial growth.[30] Tet-*O*-CMC NPs have greater activity against intracellular infection caused by *S. aureus.*[7] From the study it was confirmed that the Tet-*O*-CMC NPs are effective in reducing the bacterial growth in *S. aureus, E. coli* and their clinical strains. So the bi-layer sponge with nano Tet having good anti-bacterial activity can be effectively utilized in wound sites to prevent infection and related problems. The chitosan sponge does not show any considerable antibacterial activity when compared to bi-layer sponge with Tet-*O*-CMC NPs. It has been reported that the antibacterial activity of chitosan is negligible at neutral pH due its decreased solubility and protonation.[31] Therefore the incorporation of antimicrobial drugs and nanoparticles like silver and ZnO into chitosan based wound dressing materials is necessary to increase their antimicrobial activity effectively towards infectious wounds.[12,19,32–34]

The porcine muscle treated with Tet-*O*-CMC NPs incorporated into bi-layer sponge had shown significant reduction in bacteria compared to the bare sponge treated muscles. Since muscles are exposed to wound dressing material the delivery of drug in the muscles is more important. The nanoparticle and the released drug from the nanoparticle can penetrate through porcine muscle and can inhibit the growth of bacteria. *Ex vivo* studies provided similar results to that of *in vitro* studies. Even though the wound condition is different from the experimental setup we can say that the sponge can effectively deliver antibiotic into muscles and can decrease the bacterial load. One of the hurdles in chronic wound treatment is the control of bacterial load in the deep tissues. So our sponge can be used for the treatment of infectious chronic wounds.

The results shows that the drug loaded nanoparticles improved the penetration of the drugs. The drug can penetrate through the muscle fibres, and these nanoparticles will improve its delivery. Major factors affecting better penetration are the nano size and cationic charges. The drug permeated into the muscle treated with nanoparticles containing sponge is contributed by the penetration of nanoparticles and the drug released from the nanoparticles. The infections in the deep tissue can be easily controlled by incorporating drug loaded nanoparticles into the dressing material. Thus theses sponges can be used for infectious wounds also.

Conclusions

The chitosan–HA bi-layer sponge was prepared and characterized by SEM and FT-IR. Top layer-chitosan sponge showed about 80–85% porosity, which is an important property that is needed for an ideal wound dressing material. The highly interconnected pores will help in exudate absorption. The controlled swelling ability of chitosan sponge is also an added advantage in absorbing excess wound exudate and thus provides a moist wound atmosphere. The antifibrinolytic study showed that bi-layer sponge with amicar prevented thrombolysis as effective as amicar control and stabilized the blood clot. This confirms that the amicar present in the HA layer would be released at a faster rate. The mechanical and elongation properties confirmed the flexible and soft nature of the sponges. Tensile strength evaluation also showed that it has adequate tensile strength to be used as a dressing material. From the drug release study, it was clear that the chitosan layer having Tet-*O*-CMC NPs showed a sustained/slow drug release pattern of Tet. From the *ex vivo* muscle penetration study using porcine muscle it was found that the Tet-*O*-CMC NPs have more penetration capacity when compared to the bare drug. Antibacterial evaluation by the *ex vivo* study and using *S. aureus* and *E. coli* and their clinical strains proved that the bi-layer sponges have greater activity against both gram positive and gram negative bacteria. Cytocompatibility of bi-layer sponges was confirmed using the HDF cell line. Hence the prepared bi-layer sponge could be a promising dressing material for post-surgical/traumatic wounds in order to reduce uncontrolled bleeding under hyperfibrinolytic conditions and to prevent bacterial infection.

Acknowledgements

One of the authors Dr R. Jayakumar is grateful to the Department of Biotechnology (DBT), India, for providing funding (Ref. No. BT/PR6758/NNT/28/620/2012). Ms Annapoorna Mohandas is thankful to UGC for providing fellowship (SR. No. 2120930570). The authors are also thankful to Mr Sajin P. Ravi for his help in SEM analysis.

Notes and references

1 H. Schöchl, W. Voelckel, M. Maegele and C. Solomon, *Hamostaseologie*, 2012, **32**, 22–27.
2 B. H. Tieu, J. B. Holcomb and M. A. Schreiber, *World J. Surg.*, 2007, **31**, 1055–1064.
3 A. Giacometti, O. Cirioni, A. M. Schimizzi, M. S. Del Prete, F. Barchiesi, M. M. D'Errico, E. Petrelli and G. Scalise, *J. Clin. Microbiol.*, 2000, **38**, 918–922.
4 J. C. Cardenas, N. Matijevic, L. A. Baer, J. B. Holcomb, B. A. Cotton and C. E. Wade, *Shock*, 2014, **41**, 514–521.
5 K. Brohi, M. J. Cohen, M. T. Ganter, M. J. Schultz, M. Levi, R. C. Mackersie and J. F. Pittet, *J. Trauma*, 2008, **64**, 1211–1217.
6 B. Gunawan and B. Runyon, *Aliment. Pharmacol. Ther.*, 2006, **23**, 115–120.
7 S. Maya, S. Indulekha, V. Sukhithasri, K. T. Smitha, S. V. Nair, R. Jayakumar and R. Biswas, *Int. J. Biol. Macromol.*, 2012, **51**, 392–399.
8 R. Jayakumar, M. Prabaharan, K. P. T. Sudheesh, S. V. Nair and H. Tamura, *Biotechnol. Adv.*, 2011, **29**, 322–337.
9 A. Anitha, S. Sowmya, P. T. Sudheesh Kumar, S. Deepthi, K. P. Chennazhi, H. Ehrlich, M. Tsurkan and R. Jayakumar, *Prog. Polym. Sci.*, 2014, **39**, 1644–1667.
10 G. I. Howling, P. W. Dettmar, P. A. Goddard, F. C. Hampson, M. Dornish and E. J. Wood, *Biomaterials*, 2001, **22**, 2959–2966.

11 T. C. Santos, A. P. Marques, S. S. Silva, J. M. Oliveira, J. F. Mano, A. G. Castro and R. L. Reis, *J. Biotechnol.*, 2007, **132**, 218–226.

12 C. Chen, L. Liu, T. Huang, Q. Wang and Y. Fang, *Int. J. Biol. Macromol.*, 2013, **62**, 188–193.

13 A. Mohandas, B. S. Anisha, K. P. Chennazhi and R. Jayakumar, *Colloids Surf., B*, 2015, **127C**, 105–113.

14 M. Rinaudo, *Corros. Eng., Sci. Technol.*, 2007, **42**, 324–334.

15 B. V. Nusgens, *Ann. Dermatol. Venereol.*, 2010, **137**, S3–S8.

16 R. D. Price, S. Myers, I. M. Leigh and H. A. Navsaria, *Am. J. Clin. Dermatol.*, 2005, **6**, 393–402.

17 S. Iordanescu and M. Surdeanu, *J. Gen. Microbiol.*, 1976, **96**, 277–281.

18 P. Varma, R. K. Dinesh, K. K. Menon and R. Biswas, *J. Food Sci.*, 2010, **75**, M546–M551.

19 K. P. T. Sudheesh, V. K. Lakshmanan, T. V. Anilkumar, C. Ramya, P. Reshmi, A. G. Unnikrishnan, S. V. Nair and R. Jayakumar, *ACS Appl. Mater. Interfaces*, 2012, **4**, 2618–2629.

20 J. Guan, K. L. Fujimoto, M. S. Sacks and W. R. Wagner, *Biomaterials*, 2005, **26**, 3961–3971.

21 S. Al-Nasiry, N. Geusens, M. Hanssens, C. Luyten and R. Pijnenborg, *Hum. Reprod.*, 2007, **22**, 1304–1309.

22 N. Nataraj, G. S. Anjusree, A. A. Madhavan, P. Priyanka, D. Sankar, N. Nisha, S. V. Lakshmi, R. Jayakumar, A. Balakrishnan and R. Biswas, *J. Biomed. Nanotechnol.*, 2014, **10**, 864–870.

23 F. F. Larese, F. D'Agostin, M. Crosera, G. Adami, N. Renzi, M. Bovenzi and G. Maina, *Toxicology*, 2009, **255**, 33–37.

24 K. Sarkar, M. Debnath and P. P. Kundu, *Hydrol.: Curr. Res.*, 2012, **3**, 138, DOI: 10.4172/2157-7587.1000138.

25 J. Li, X. Wang, X. Liu, X. Zhuang, X. Wu and J. Li, *Fibers Polym.*, 2014, **15**, 1575–1582.

26 S. Gunasekaran, S. R. Varadhan and N. Karunanidhi, *Proc. Indian Natn. Sci. Acad.*, 1996, **62**, 309–316.

27 A. Abdulkarim, M. T. Isa, S. Abdulsalam, A. J. Muhammad and A. O. Ameh, *Civil Environ. Res.*, 2013, **3**, 108–114.

28 C. R. Correia, L. S. Moreira-Teixeira, L. Moroni, R. L. Reis, C. A. van Blitterswijk, M. Karperien and J. F. Mano, *Tissue Eng., Part C*, 2011, **17**, 717–730.

29 D. P. Jayesh, M. Frej, A. Abdellah and E. Saïd, *Mater. Sci. Appl.*, 2012, **3**, 125–130.

30 I. Chopra and M. Roberts, *Microbiol. Mol. Biol. Rev.*, 2001, **65**, 232–260.

31 C. Qin, H. Li, Q. Xiao, Y. Liu, J. Zhu and Y. Du, *Carbohydr. Polym.*, 2006, **63**, 367–374.

32 D. H. Li, J. L. Diao, J. T. Zhang and J. C. Liu, *J. Nanosci. Nanotechnol.*, 2011, **11**, 4733–4738.

33 K. Vimala, Y. M. Mohan, K. S. Sivudu, K. Varaprasad, S. Ravindra, N. N. Reddy, Y. Padma, B. Sreedhar and K. Mohana Raju, *Colloids Surf., B*, 2010, **76**, 248–258.

34 P. T. S. Kumar, V. K. Lakshmanan, R. Biswas, S. V. Nair and R. Jayakumar, *J. Biomed. Nanotechnol.*, 2012, **8**, 891–900.